Scientia Pharmaceutica

ÖSTERREICHISCHE PHARMAZEUTISCHE GESELLSCHAFT

MDPI

Article

Antineoplastic Activity of Water-Soluble Form of Novel Kinase Inhibitor 1-(4-Chlorobenzyl)-3-chloro-4-(3-trifluoromethylphenylamino)-1*H*-pyrrole-2,5-dione immobilized on Polymeric Poly(PEGMA-*co*-DMM) Carrier

Nataliya Finiuk [1], Olga Klyuchivska [1], Nataliya Mitina [2], Halyna Kuznietsova [3], Kateryna Volianiuk [2], Alexander Zaichenko [2], Volodymyr Rybalchenko [3] and Rostyslav Stoika [1,3,*]

[1] Institute of Cell Biology, National Academy of Sciences of Ukraine, 79005 Lviv, Ukraine; nataliyafiniuk@gmail.com (N.F.); zorepad1775@gmail.com (O.K.)
[2] Department of Organic Chemistry, Institute of Chemistry and Chemical Technologies, Lviv Polytechnic National University, 79013 Lviv, Ukraine; nmitina10@gmail.com (N.M.); k.volianiuk@gmail.com (K.V.); alzaich@i.ua (A.Z.)
[3] Institute of High Technologies, Taras Shevchenko National University of Kyiv, 01601 Kyiv, Ukraine; biophyz@gmail.com (H.K.); v.k.rybalchenko@gmail.com (V.R.)
* Correspondence: stoika.rostyslav@gmail.com; Tel.: +380-32-261-2287

Citation: Finiuk, N.; Klyuchivska, O.; Mitina, N.; Kuznietsova, H.; Volianiuk, K.; Zaichenko, A.; Rybalchenko, V.; Stoika, R. Antineoplastic Activity of Water-Soluble Form of Novel Kinase Inhibitor 1-(4-Chlorobenzyl)-3-chloro-4-(3-trifluoromethylphenylamino)-1*H*-pyrrole-2,5-dione immobilized on Polymeric Poly(PEGMA-*co*-DMM) Carrier. *Sci. Pharm.* **2022**, *90*, 7. https://doi.org/10.3390/scipharm90010007

Academic Editor: Claudio J. Salomón

Received: 3 December 2021
Accepted: 13 January 2022
Published: 21 January 2022

Abstract: The maleimide derivative 1-(4-chlorobenzyl)-3-chloro-4-(3-trifluoromethylphenylamino)-1*H*-pyrrole-2,5-dione (MI-1) was synthesized as inhibitor of several protein kinases, however, its application is hindered by its poor water solubility. In this study, the mechanisms of the antineoplastic action of MI-1 and its MI-1/M5 complex with M5 carrier (poly (PEGMA-*co*-DMM)) towards human colon carcinoma HCT116 cells were investigated by using the MTT and clonogenic assays, DNA intercalation with methyl green replacement, alkaline DNA comet assay, and Western-blot analysis. MI-1 compound and its MI-1/M5 complex possessed high toxicity towards colon (HCT116), cervical (HeLa) carcinoma cells and melanoma (SK-MEL-28) cells with GI_{50} value in a range of 0.75–7.22 μg/mL, and demonstrated high selectivity index (SI 6.9). The p53 status of colon cancer cells did not affect the sensitivity of these cells to the treatment with MI-1 and its MI-1/M5 complex. M5 polymer possessed low toxicity towards studied cells. The MI-1, MI-1/M5, and M5 only slightly inhibited growth of the pseudo-normal HaCaT and Balb/c 3T3 cell lines (GI_{50} 50 μg/mL). The MI-1 and its MI-1/M5 complex induced mitochondria-dependent pathway of apoptosis, damage of the DNA, and morphological changes in HCT116 cells, and affected the G2/M transition checkpoint. The MI-1 intercalated into the DNA molecule, while such capability of MI-1/M5 complex and M5 polymer was much lower. Thus, poly (PEGMA-*co*-DMM) might be a promising carrier for delivery of the maleimide derivative, MI-1, a novel kinase inhibitor, through improving its solubility in aqueous media and enhancing its antiproliferative action towards human tumor cells. Studies are in progress on the treatment of Nemeth-Kellner lymphoma (NK/Ly)-bearing mice with the MI-1 and MI-1/M5 complex.

Keywords: 1*H*-pyrrole-2,5-diones; polymeric carrier; cytotoxicity; tumor cells; apoptosis; DNA damage

1. Introduction

Despite big progress in studying the multistep process of carcinogenesis as a genetic disorder with the implication of different cell signaling mechanisms, as well as the extensive research aimed at the creation of selective and effective anticancer agents [1], serious problems still exist in cancer treatment. These problems are mainly caused by the rapid development of multidrug resistance in malignant cells, poor bio-availability and adverse effects of anticancer medicines, and poor water solubility of drugs [2]. Application of nanomaterials and nanobiotechnologies is an effective approach for the improvement of

the solubility and therefore therapeutic efficacy of anticancer drugs [3,4]. Several types of the polymeric nanocarriers were proposed for drug delivery, e.g., poly (lactic-*co*-glycolic acid) (PLGA), poly (lactic acid) (PLA), poly (ethylene glycol) (PEG), poly(vinylpyrrolidone), poly(ε-caprolactone) (PCL), poly (ethylene oxide) (PEO), various micellar materials, hybrid copolymers, lipid-based carriers, and others [5–9].

On the other hand, a search for new natural or synthetic substances that possess anticancer action continues with the hope of detecting highly specific agents for targeting tumor cells with minimal harm for normal tissues and organs of the body. Hybrid heterocyclic molecules demonstrated several pharmaceutical activities that attract the interest of researches. Maleimide is a bioactive molecule which possesses a stability, electrophilic properties, and selectivity of action. It is used for bio-conjugation of oligonucleotides, peptides and proteins [10,11], for preparation of self-healing systems, thermostable materials, and applied in click reactions [12]. Maleimide derivatives were reported as antimicrobial agents towards *Staphylococcus aureus*, *Escherichia coli*, *Aspergillus niger*, *Mycobacterium tuberculosis* [13]. N-substituted maleimides (N-phenylsuccinimide, N-phenylphtalimide, 2,3-dimethylmaleic anhydrides) acted as monoglyceride lipase inhibitors [14]. Bis-indolylmaleimides [15], aryl-indolyl maleimides [16] and indolyl-naphthyl maleimides [17] have been shown to inhibit protein kinases, glycogen synthetase kinase-3 (GSK-3) and different isoforms of protein kinase C (PKC). The maleimide-PEG was used as a linker for the conjugation of S2P peptide to PLGA nanoparticles [18]. Besides, it was applied for functionalization of Pt (IV) complexes [19] and for delivery and release of IL-1Ra [20]. Hu et al. synthesized the maleimide-functionalized poly-*p*-xylylenes via a maleimide–thiol coupling reaction and characterized them as robust bioengineering materials [21]. The bis-maleimide enhanced the mechanical properties of the furan-functionalized polymer (FEEMA64) through the Diels-Alder reaction [22].

The maleimide derivate 1-(4-chlorobenzyl)-3-chloro-4-(3-trifluoromethylphenylamino)-1*H*-pyrrole-2,5-dione (MI-1) was designed in silico and it was proposed as an ATP-competitive, type I inhibitor of tyrosine kinases [23,24]. The MI-1 also demonstrated the anti-inflammatory activity [25]. The anti-cancer activity of the MI-1 was shown in the in vitro [24,26–28] and in vivo experiments [29–32]. However, poor water solubility remains a big drawback of the biomedical application of the MI-1 that hinders its application as a medicinal remedy. We suggest that the biggest progress in the biomedical use of the maleimide as a bioactive molecule would be achieved via solving the bio-availability problem, and not via development of new derivatives of this agent.

In this study, we created a water-soluble form of novel kinase inhibitor, MI-1. To reach this goal, we immobilized MI-1 on the polymeric carrier poly (PEGMA-*co*-DMM) (M5) which demonstrated its effectiveness in the delivery of the experimental anticancer agent–thiazole derivative N-(5-benzyl-1,3-thiazol-2-yl)-3,5-dimethyl-1-benzofuran-2-carboxamide [33]. In order to approve the anticancer action in vitro of the created complex of MI-1 immobilized on the poly (PEGMA-*co*-DMM) carrier, a set of experiments aimed at the investigation of cellular and molecular mechanisms of the antineoplastic action of this complex were conducted with targeting human colon carcinoma cells of HCT116 line. The main reason of such selection of cells was based on the results of our former studies which demonstrated high effectiveness of the MI-1 in treatment of disorders of gastro-intestinal tract (e.g., inflammation) [24,25,29,30]. Here, we found that the immobilization of the MI-1 on the carrier poly (PEGMA-*co*-DMM) provided a creation of a water-soluble form of MI-1, and also enhanced the antineoplastic action in vitro of the MI-1.

2. Materials and Methods

2.1. Studied Compounds

2.1.1. Synthesis and Characterization of Maleimide Derivative

The maleimide derivative MI-1 (1-(4-chlorobenzyl)-3-chloro-4-(3-trifluoromethylphenylamino)-1*H*-pyrrole-2,5-dione) (Figure 1) was synthesized via chemical transformations, as described previously [24,34]. Briefly, the para-chlorobenzylamine was added to the solution of 3,4-dichlorofuran-

2,5-dione in ice acetic acid. After that, the appropriate aromatic amine was added and the mixture was boiled with ethyl alcohol. Control of the reaction effectiveness was carried out by thin-layer chromatography. After finishing of the reaction, the solvent was evaporated in vacuo. Product was filtered and washed with ethanol and a small amount of cold water. The product was purified by recrystallization on silica gel (230–400 mesh) using hexane/ethyl acetate (7:3) solution as the eluent. The MI-1 structure was confirmed by 1H and 13C spectra [24].

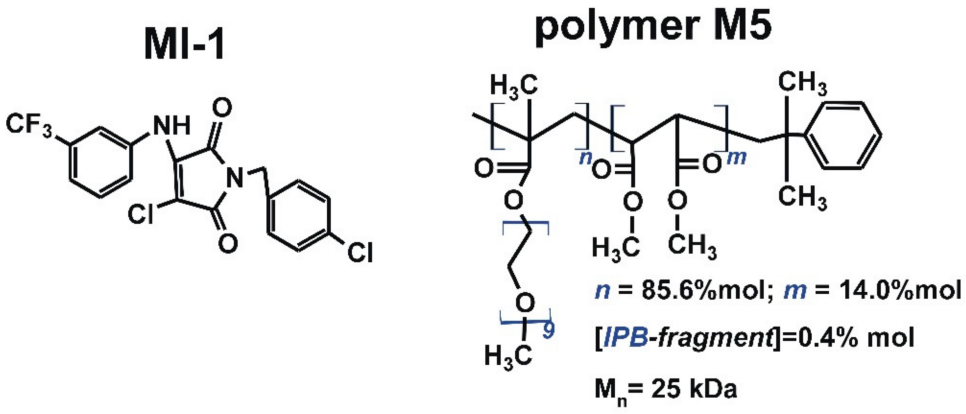

Figure 1. The structure of (**a**) maleimide derivative MI-1 (1-(4-chlorobenzyl)-3-chloro-4-(3-trifluoromethylphenylamino)-1*H*-pyrrole-2,5-dione) and (**b**) polymeric carrier poly (PEGMA-*co*-DMM) (M5) [24,33].

The MI-1 was dissolved in the Dimethyl Sulfoxide (DMSO, Sigma-Aldrich, St Louis, MO, USA) to obtain the stock solution of 10 mg/mL. The subsequent dilutions of the MI-1 were done in the culture medium.

2.1.2. Synthesis and Characterization of the Polymeric Carrier

The polymeric carrier poly (PEGMA-*co*-DMM) (M5, Figure 1) was synthesized at the Department of Organic Chemistry of Lviv Polytechnic National University (Ukraine). The following reagents were used to synthesize the polymer carrier M5: dimethyl maleate (DMM) (Acros Organics, Waltham, MA, USA) was purified by distillation in vacuum; polyethylene glycol methyl ether methacrylate (PEGMA, Mn = 475 Da), azobis(isobutyronitrile) (AIBN), isopropylbenzene (IPB) and 1,4-dioxane were obtained from Sigma-Aldrich (St Louis, MO, USA) and used without additional purification.

The comb-like poly (PEGMA-*co*-DMM) (M5) carrier was synthesized in dioxane via radical copolymerization of PEGMA with DMM initiated by AIBN in the presence of IPB as the chain transfer agent for controlling polymer chain length [35]. A mixture of PEGMA (3.8 mL, 8.0 mmol) and DMM (0.13 mL, 0.9 mmol) and 10 mL of the IPB (0.03 mL, 0.3 mmol was prepared, then AIBN (0.1 g, 0.61 mmol) solution in dioxane was added to the mixture. The synthesis was carried out at 333 K until 65% of monomer conversion. Then copolymer was separated from the final mixture and purified by multiple re-precipitations from solution into hexane. Residual PEGMA was removed by dialysis using dialysis bags with pore sizes MWCO 6–8 kDa (Sigma-Aldrich, St Louis, MO, USA). The resulting polymers were dried under vacuum until a constant weight [36].

2.1.3. Synthesis and Characterization of the Complex of Maleimide Derivative with Polymer

The polymer M5 and MI were dissolved in the DMSO, and the solutions were subsequently transferred in water to form the complexes of MI-1 and polymer M5. Initially, 45 mg of polymer was dissolved in 0.15 mL of DMSO and 1.5 g of MI-1 was dissolved in 0.1 mL of DMSO. The polymer M5 and MI-1 solutions were mixed, added to 4.25 mL of

Saline, and subjected to ultrasound (US) dispersion for 10 s. The solution of free polymer M5 was prepared by dilution of 45 mg of PC in 0.45 mL of DMSO. Next, it was added to the 4.0 mL of physiological solution and subjected to the ultrasound dispersion for 10 s [37], as a result, stable colloidal systems were formed (Figure 2). The size of M5 polymer micelles and drug-filled micellar structures of MI-1/M5 complex was determined by dynamic light scattering method (DLS) that was performed using a DynaPro NanoStar (Wyatt Technology, Santa Barbara, CA, USA).

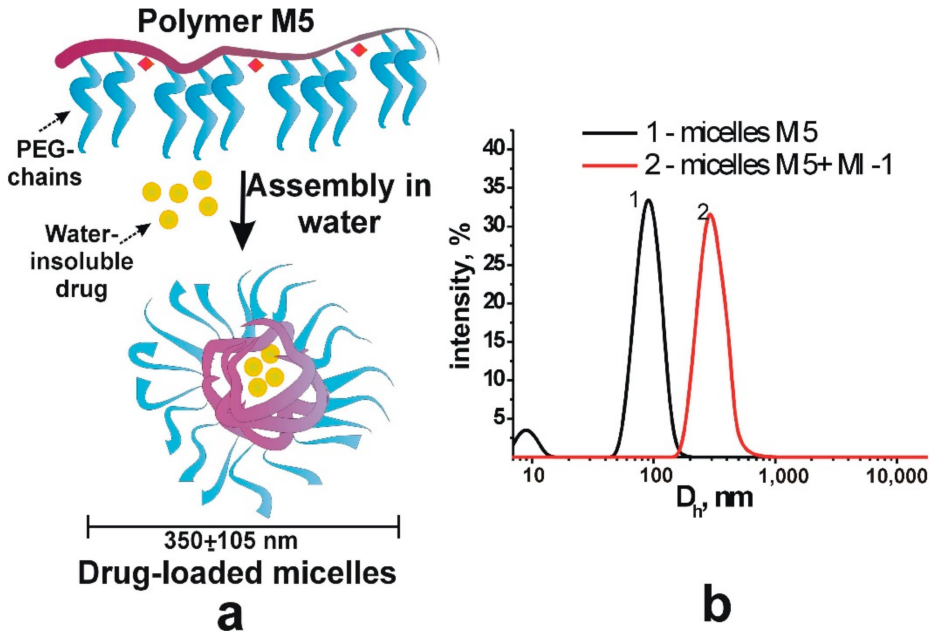

Figure 2. Scheme (**a**) of the formation of stable micellar structures filled with drugs and (**b**) hydrodynamic diameter of polymer micelles M5 and drug-filled micellar structures (M5 + MI-1).

2.1.4. Doxorubicin

The Doxorubicin (Dox, Actavis S.R.L., Bucharest, Romania) was used as the reference anticancer drug.

2.2. Cell Culture

Human colon carcinoma HCT116 cells, human cervical adenocarcinoma HeLa cells, and human melanoma SK-MEL-28 cells, human HaCaT keratinocytes, and murine Balb/c 3T3 fibroblasts were obtained from the Institute of Experimental Pathology, Oncology and Radiobiology (Kyiv, Ukraine) which received those cells from the ATCC (American Type Culture Collection). The p53-deficient HCT116 p53-/- colon cancer cells were donated by a Collection of the Institute for Cancer Research at Vienna Medical University (Vienna, Austria). HCT116 and HCT116 p53-/- cells were cultivated in the RPMI-1640 medium, SK-MEL-28 and HeLa cells–in the DMEM medium. Culture medium was supplemented with 10% of fetal bovine serum (all were purchased from Biowest, Nuaille, France) at 37 °C in atmosphere of 95% air and 5% CO_2 [38].

2.3. The MTT Assay

The functional activity of cells treated with compound MI-1, complex MI-1/M5, polymer M5, doxorubicin, and DMSO was measured using the MTT (3-(4,5-dimethyl thiazol-2-yl)-2,5-diphenyl tetrazolium bromide, Sigma-Aldrich, St Louis, MO, USA) assay according to the manufacturer's recommendations (Sigma-Aldrich, St Louis, MO, USA), as described [27]. Briefly, the MI-1, MI-1/M5 complex, polymer M5 (1, 10, and 100 μg/mL) or doxorubicin (1, 10 μg/mL) was added in 100 μL of the cultural medium, and cells were incubated for the next 72 h. The absorbance of formazan was measured by an Absorbance

Reader BioTek ELx800 (BioTek Instruments, Inc., Winooski, VT, USA). The initial value of the relative number of cells in control (under 0 μg/mL of compounds) was accepted as 100%. The half growth inhibition (GI_{50}) value of studied compounds was calculated as the drug concentration that reduced cell viability by 50%.

2.4. The Clonogenic Assay

The clonogenic assay was conducted using the modified protocol described previously [39]. The HCT116 cells (750 cells/1 mL) were seeded in a 12-well plate. After adhesion, cells were treated with the MI-1, MI-1/M5, M5 or doxorubicin (all at 0.1; 0.25; 0.5; 1.0 μg/mL) for 7 days. Then, the cells were washed with the phosphate buffered saline (PBS), fixed with cold methanol for 10 min. Cells were stained with 0.5% crystal violet dye in 25% methanol for 10 min. Cells were washed with the PBS. The colonies were counted using ImageJ software as open source.

2.5. The Western-Blot Analysis

The concentration 0.9 μg/mL of MI-1, complex MI-1/M5, polymer M5, and Dox was chosen as working dose at Western-blot analysis of their pro-apoptotic effects in HCT116 cells. We used the modified protocol of the Western-blot assay [40]. Cellular proteins were extracted with lysis buffer (20 mM Tris-HCl, pH 8.0, 1% Triton-X100, 150 mM NaCl, 50 mM NaF, 0.1% SDS) containing 1 mM phenylmethanesulfonyl fluoride (PMSF) and 10 μg/mL of protease inhibitors cocktail "Complete" (Roche, Basel, Switzerland). Proteins (30 μg/lane) were separated by the SDS/PAGE gel-electrophoresis and transferred onto a polyvinylidene difluoride (PVDF) membrane [38].

The primary antibodies against a Cleaved Caspase 3 (Asp175), EndoG, Apaf1, phosphorylated form of MAPK, Cdk2, Cdk4, Bax, Bcl-2, phosphorylated Chk2, phosphorylated STAT1, beta-actin (Cell Signaling Technology, Vienna, Austria) were used. Secondary peroxidase-conjugated antibodies (Cell Signaling Technology, Vienna, Austria) were applied at a working dilution of 1:5000 according to the manufacture's recommendations. The enhanced chemiluminescence (ECL) detection reagent (Sigma-Aldrich, St Louis, MO, USA) was used for protein visualization. The densitometric analysis of protein content was conducted using the ImageJ software as open source [41].

2.6. The DNA Intercalation Assay Using Methyl Green Replacement

The ability of the tested compounds to intercalate into DNA was estimated using the methyl green replacement assay according to [27]. Methyl green binds to DNA forming the complex with an absorption maximum at 642 nm. Free methyl green does not show absorption at this wavelength. The compounds that intercalate into DNA replaced methyl green from the complex of methyl green-DNA and decreased the optical density at 642 nm. Briefly, salmon sperm DNA (50 μg/mL, Sigma-Aldrich, St Louis, MO, USA) was incubated for 1 h at 37 °C with 15 μL methyl green (1 mg/mL, Sigma-Aldrich, St Louis, MO, USA). The absorbance of methyl green was measured after incubation of methyl green-DNA with MI-1, MI-1/M5, M5, Ethidium bromide (EtBr, Sigma-Aldrich, St Louis, MO, USA) (all at 1 and 10 μg/mL), or doxorubicin (1 μg/mL) for next 1 h at 37 °C using a fluorescence plate reader (Absorbance Reader BioTek ELx800, BioTek Instruments, Inc., Winooski, VT, USA).

2.7. The Comet Assay at Alkaline Conditions

DNA comet assay at the alkaline conditions was performed, as described [38]. Briefly, the HCT116 cells were seeded in 12-well plates at a concentration of 50,000 cells/1 mL, and after 24 h, cells were treated for the next 24 h with the studied compounds at 0.9 μg/mL. The 25,000 of cells in 100 μL of 0.5% low melting agarose (Promega, Madison, WI, USA) was transfer to the frosted microscopic slides covered with 1% normal molten agarose (LACHEMA, Prague, Czech Republic). Cell were lysed for 4–6 h at 4 °C in the lysis buffer (2.5 M NaCl; 100 mM EDTA; 10 mM Tris, pH 10.0; 10% DMSO, 1% Triton X-100). Electrophoresis was performed at 25 V for 25 min in electrophoresis solution (1 mM EDTA;

300 mM NaOH, pH 13.0) at 4 °C. After that, slides were stained with Ethidium bromide (10 μg/mL, Sigma Aldrich, St Louis, MO, USA) and visualized using a Zeiss fluorescent microscope and AxioImager A1 camera. Images were additionally analyzed using Casplab-1.2.3b2 software to calculate the olive tail moment (OTM, the product of the tail length and the fraction of total DNA in the tail) [38].

2.8. The Fluorescent Microscopy of Cells

The HCT116 cells were seeded on glass microscopic slides in 12-well plates, and then treated for 24 h with studied compounds at 0.25 μg/mL and/or 1 μg/mL and analyzed using a Zeiss fluorescent microscope (Carl Zeiss, Jena, Germany) and AxioImager A1 camera (400× magnification), as described previously [38]. Cells were additionally incubated for 20–30 min with Hoechst-33342 dye (0.5 μg/mL, Sigma-Aldrich, St Louis, MO, USA). Propidium iodide (PI, 20 μg/mL, Sigma-Aldrich, St Louis, MO, USA) was added immediately before microscopic cells examination. All microphotographs were additionally analyzed using ImagePro7 software [38].

2.9. Statistical Analysis

The results were analyzed and illustrated using GraphPad Prism (version 6; GraphPad Software, La Jolla, CA, USA), and presented as a mean ± standard deviation. ANOVA test (by Dunnett's test) or t test was used for statistical analysis. Statistical significance was identified at $p \leq 0.05$.

3. Results and Discussions

3.1. The Viability of Tumor and Pseudo-Normal Cells after Treatment

At the first stage of study, we have investigated the cytotoxicity in vitro of the maleimide derivative MI-1 complexed with the polymeric carrier poly (PEGMA-*co*-DMM) towards tumor and pseudo-normal cells. It was established that the studied compound and its complex with the polymeric carriers differ in the antiproliferative action on tumor cells (Figure 3). We found that MI-1 compound and MI-1/M5 complex possessed significant cytotoxic action toward colon carcinoma, cervical carcinoma, and melanoma cells. The MI-1 inhibited growth of HCT116 cells with the GI_{50} of 0.75 μg/mL, complex MI-1/M5–with the GI_{50} of 0.67 μg/mL (Figure 3, Table 1). The mutations in tumor suppressor gene *TP53* that encoded the p53 protein are widely spread in colorectal cancer [42]. The *P53* mutation stimulated hyper-proliferation and chemo-resistance of tumor cells and enhanced invasion/metastasis [43]. The anti-cancer efficacy of oxaliplatin, 5-FU, cisplatin depended on the p53 status in tumor cells [44,45]. The GI_{50} value of the MI-1 for human colon carcinoma HCT116 p53-/- cells with the deletion of *P53* gene equaled 0.89 μg/mL. The MI-1/M5 complex was more toxic ($p \leq 0.01$) for the HCT116 p53-/- cells than free form of the MI-1. Thus, *P53* gene status in colon carcinoma HCT116 cells does not affect the sensitivity of these cells to the treatment with maleimide derivative MI-1 and the MI-1/M5 complex.

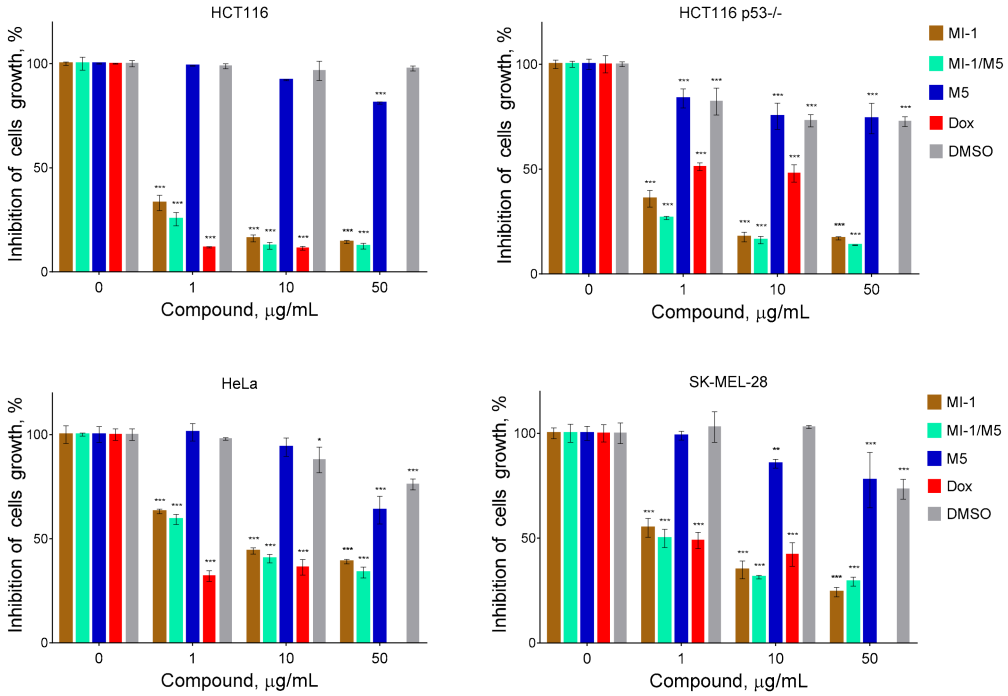

Figure 3. The cytotoxicity of MI-1 maleimide derivative, its complex MI-1/M5 with polymeric carrier, free polymeric carrier poly (PEGMA-*co*-DMM) (M5), doxorubicin (Dox), and solvent DMSO towards human colon carcinoma HCT116 and HCT116 p53-/- cells, human cervical adenocarcinoma HeLa cells, and human melanoma SK-MEL-28 cells. The effect was measured by the MTT assay under 72 h cell exposure. Data are presented as the mean ± SD. * $p < 0.05$; ** $p < 0.01$; *** $p < 0.001$ compared with control (non-treated) cells.

Table 1. The cytotoxicity (GI_{50}) value of studied compounds towards the mammalian cells (MTT assay, 72 h of treatment).

Cell Line	IC_{50}, μg/mL				
	MI-1	**MI-1/M5**	**M5**	**Dox**	**DMSO**
Tumor cells					
HCT116	0.75 ± 0.06	0.67 ± 0.06	50	0.58 ± 0.04 *	50
HCT116 p53-/-	0.89 ± 0.05	0.68 ± 0.05 **	50	3.60 ± 0.51 ***	50
HeLa	7.22 ± 0.32	5.43 ± 0.30 **	50	0.64 ± 0.03 ***	50
SK-MEL-28	3.17 ± 0.18	1.00 ± 0.08 ***	50	0.98 ± 0.07 ***	50
Pseudo-normal cells					
HaCaT	50	50	50	1.04 ± 0.07	50
Balb/c 3T3	50	50	50	0.90 ± 0.07	50

Comments: * $p < 0.05$; ** $p < 0.01$; *** $p < 0.001$ compared with the effect of MI-1.

The GI_{50} of MI-1/M5 in HeLa cells equaled 5.43 μg/mL, while the GI_{50} of MI-1 in these cells was 7.22 μg/mL (Table 1). MI-1/M5 complex was more toxic ($p \leq 0.01$) for the SK-MEL-28 cells than the MI-1, and the GI_{50} of MI-1 was 3.17 μg/mL, while the GI_{50} of MI-1/M5 was 1.00 μg/mL. It is worth noting that tested tumor cells were resistant to treatment with free polymeric carrier (M5) or DMSO and the GI_{50} 50 μg/mL (Figure 3, Table 1). While a known chemotherapeutic agent, doxorubicin, possessed high toxicity towards HCT116, HCT116 p53-/-, HeLa, and SK-MEL-28 cells with the GI_{50} value of 0.58 μg/mL, 3.60 μg/mL, 0.64 μg/mL, 0.98 μg/mL, respectively.

It should be noted that the pseudo-normal cells of HaCaT and Balb/c 3T3 lines were relatively resistant (GI_{50} 50 μg/mL) to the inhibitory action of the maleimide derivative MI-1, its complex with polymeric carrier (MI-1/M5), and the polymeric carrier poly (PEGMA-*co*-DMM) (M5) (Figure 4, Table 1). Meanwhile the GI_{50} of doxorubicin for these non-malignant was 1.04 μg/mL and 0.90 μg/mL, respectively. García [46] reported about the cytocompatibility and minimal adverse effects of PEG-maleimide hydrogels used as the vehicles for proteins in cells.

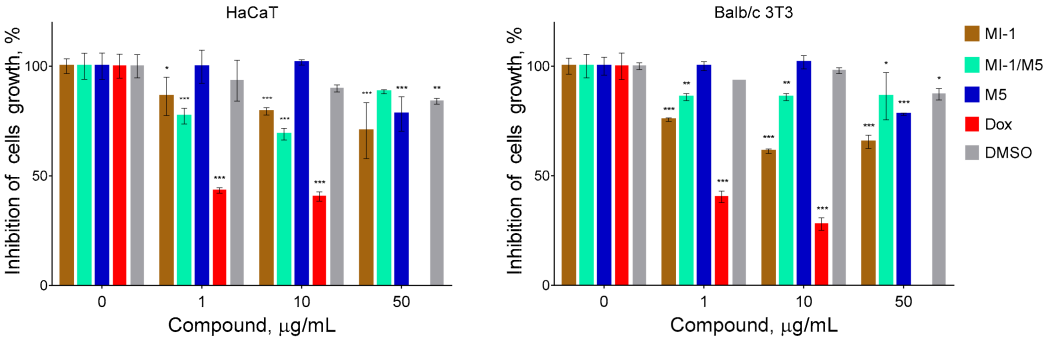

Figure 4. The cytotoxicity of maleimide derivative MI-1, its complex MI-1/M5 with polymeric carrier, free polymeric carrier poly (PEGMA-*co*-DMM) (M5), doxorubicin (Dox), and solvent DMSO towards pseudo-normal cells: human keratinocytes of HaCaT line and murine fibroblasts of Balb/c 3T3 line. The effect was measured by the MTT assay under 72 h cell exposure. Data are presented as the mean ± SD. * $p < 0.05$; ** $p < 0.01$; *** $p < 0.001$ compared with control (non-treated) cells.

The selectivity of action of chemopreventive agents is an important parameter of the pharmaceuticals that identifies their clinical potential. The higher selectivity index (SI) of compound indicates greater anticancer specificity and efficiency in cancer chemotherapy, as well as higher safety (smaller toxic effect towards normal cells) [39,47]. The compounds displaying the SI > 3.0 are considered to be highly selective [48]. The MI-1 compound and the MI-1/M5 complex demonstrated high selectivity (SI 6.9) towards human tumor cells of HCT116, HCT116 p53-/-, HeLa, and SK-MEL-28 lines (Table 2), while the M5 polymer showed low selectivity for these cancer cells. It should be noted that doxorubicin is less selective for all tested tumor cells (SI < 1.8). Thus, the MI-1 compound and the MI-1/M5 complex demonstrated more selective cytotoxic action towards cancer cells compared with the doxorubicin.

Table 2. The selectivity index (SI) of the studied compounds towards human tumor cells of different lines.

Cell Line	Selectivity Index				
	MI-1	**MI-1/M5**	**M5**	**Dox**	**DMSO**
HCT116	66.67	74.63	1.00	1.79	1.00
HCT116 p53-/-	56.18	73.53	1.00	0.29	1.00
HeLa	6.93	9.21	1.00	1.63	1.00
SK-MEL-28	15.77	50.00	1.00	1.06	1.00

Comment: The SI was calculated as the ratio GI_{50} (non-tumoral cells of HaCaT line)/GI_{50} (selected line of tumoral cells).

3.2. Clonogenic Response of Human Colon Carcinoma Cells to Treatment

The colony-forming capacity of cancer cells is an important parameter used for estimation of the anticancer activity of studied agents. Its measurement permits defining the fraction of tumor cells that retains a capacity to produce colonies that is an important phenotypic characteristics of tumor cells [39,49]. MI-1 compound in 0.1 μg/mL dose decreased (by 31.5%) the number of colonies formed by the carcinoma cells of HCT116 line

from 162 (control) to 111, in 0.25 μg/mL dose–to 72 (by 55.6%), in 0.5 μg/mL dose–to 1 (by 99.4%), and in 1 μg/mL dose, there were no colonies of tumor cells detected (Figure 5). The MI-1/M5 complex demonstrated an even more steep inhibition of the formation of colonies of HCT116 cells depending on its dose. The colony inhibitory effects of the M5 polymer and DMSO were rather weak. Doxorubicin (positive control) applied in 0.1 μg/mL dose, inhibited the formation of colonies of HCT116 cells by 50.6% (80 units), in 0.25 μg/mL dose–by 89.5% (17 units), and 0.5 μg/mL and 1 μg/mL doses fully stopped colony formation (Figure 5).

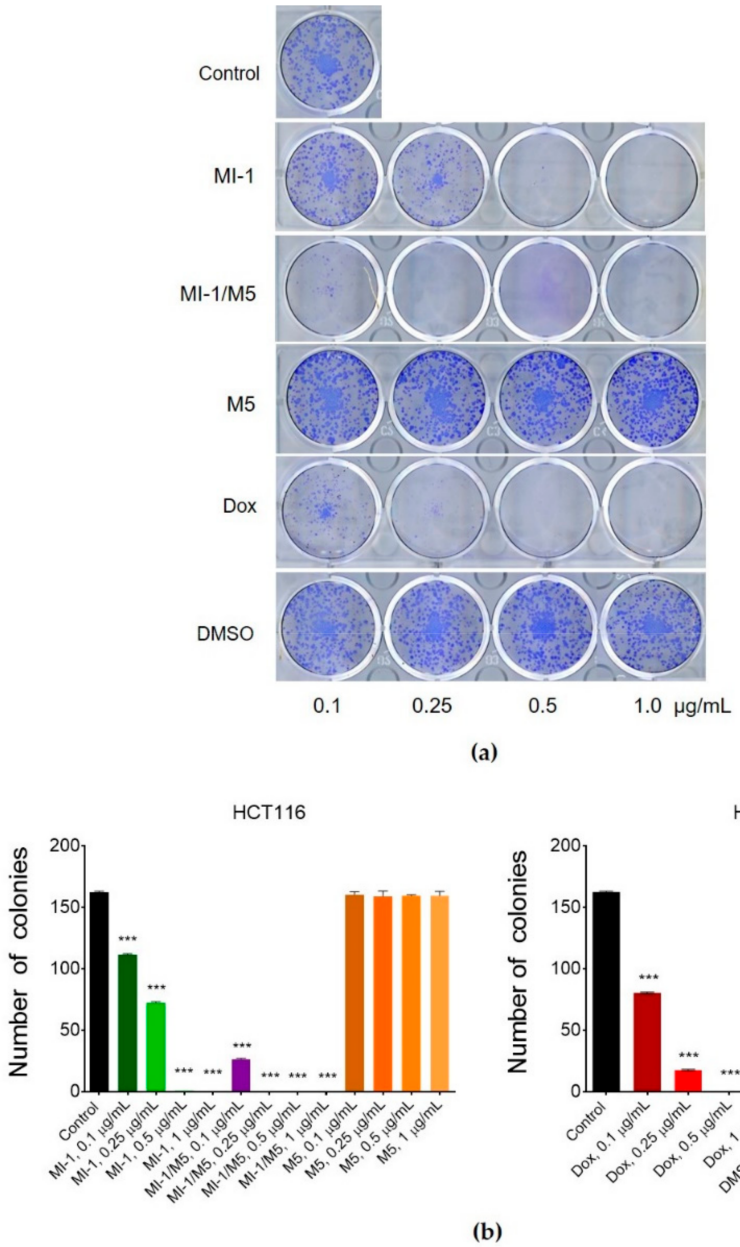

Figure 5. The effect of maleimide derivative MI-1, its complex with polymeric carrier (MI-1/M5), free polymeric carrier poly (PEGMA-*co*-DMM) (M5), doxorubicin (Dox), and solvent DMSO on clonogenic ability of HCT116 cells under 7 days of cells exposure: (**a**) The representative pictures of colonies formed in the 12-well plates; (**b**) Number of colonies formed by HCT116 cells. Data are presented as the mean ± SD. *** $p < 0.001$ compared with control (non-treated) cells.

Thus, the MI-1/M5 complex was more efficient compared with free MI-1 in suppression of the malignant phenotype (colony formation) of human colon carcinoma HCT116 cells.

3.3. Apoptosis Induction in Treated Cells

The potential mechanisms of cytotoxic action of the MI-1 compound, its MI-1/M5 complex with poly (PEGMA-*co*-DMM), and M5 polymer in HCT116 cells were investigated by using Western-blot analysis. It was found that the MI-1, MI-1/M5 complex, and doxorubicin induced an increase in the content of active (cleaved) form of caspase 3 in treated HCT116 cells. M5 polymer did not change the content of cleaved caspase 3 in these cells (Figures 5 and 6). The effector caspases, in particular caspase 3, are known to cleave various intracellular molecular targets that regulate the metabolism of DNA, histones and other proteins [50].

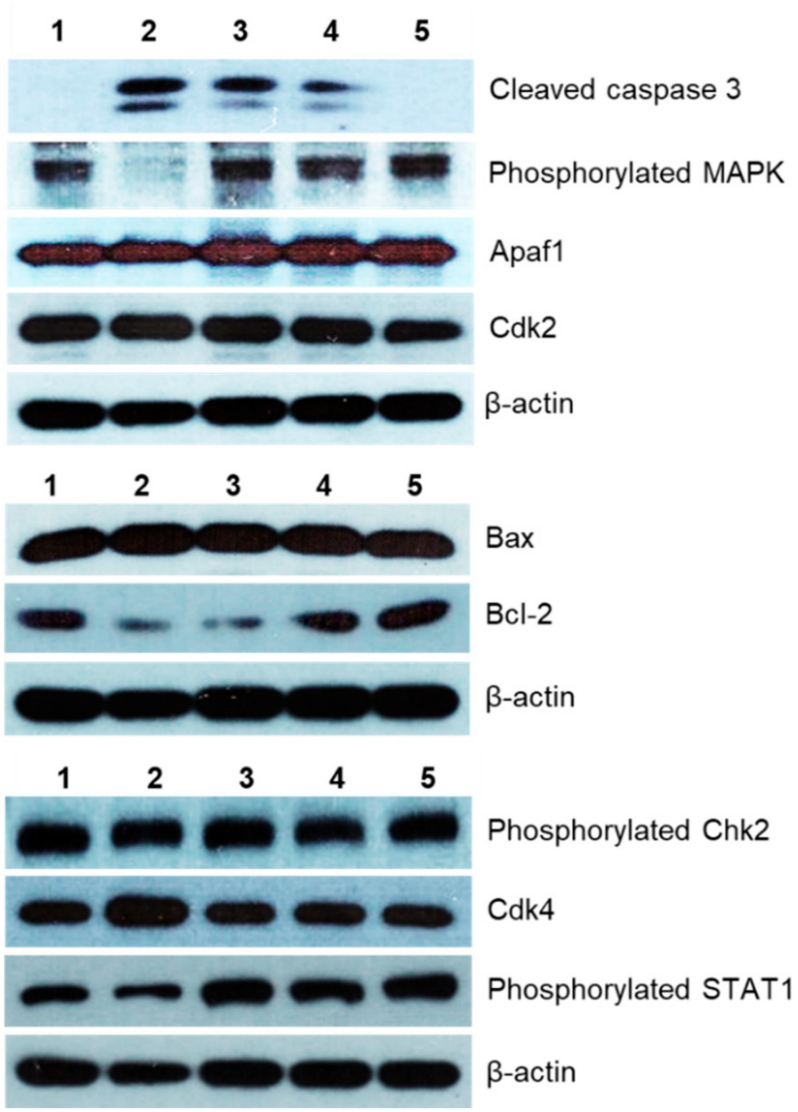

Figure 6. The level of apoptosis- and cell cycle-associated proteins in HCT116 cells after 48 h treatment with different agents (Western-blot analysis data): 1–control (non-treated) cells, 2–doxorubicin (Dox, 0.9 μg/mL), 3–MI-1 (0.9 μg/mL), 4–MI-1/M5 complex (0.9 μg/mL), 5–poly (PEGMA-*co*-DMM) polymeric carrier (M5) (0.9 μg/mL).

The creation of antitumor agents that cause mitochondrial changes and therefore could initiate mitochondria-dependent apoptotic signaling pathway is a promising strategy for the development of targeted antitumor chemotherapy [49–51]. The level of Bcl-2 (inhibitor of apoptosis) and Bax (inducer of apoptosis) proteins, as well as of the Apaf1 protein were measured. We found that the MI-1, MI-1/M5 complex, and doxorubicin reduced the

amount of the Bcl-2 protein and increased the amount of Bax protein in the treated HCT116 cells. However, there were no changes in the amount of Bcl-2 and Bax proteins in HCT116 cells treated with free M5 polymer (Figures 6 and 7).

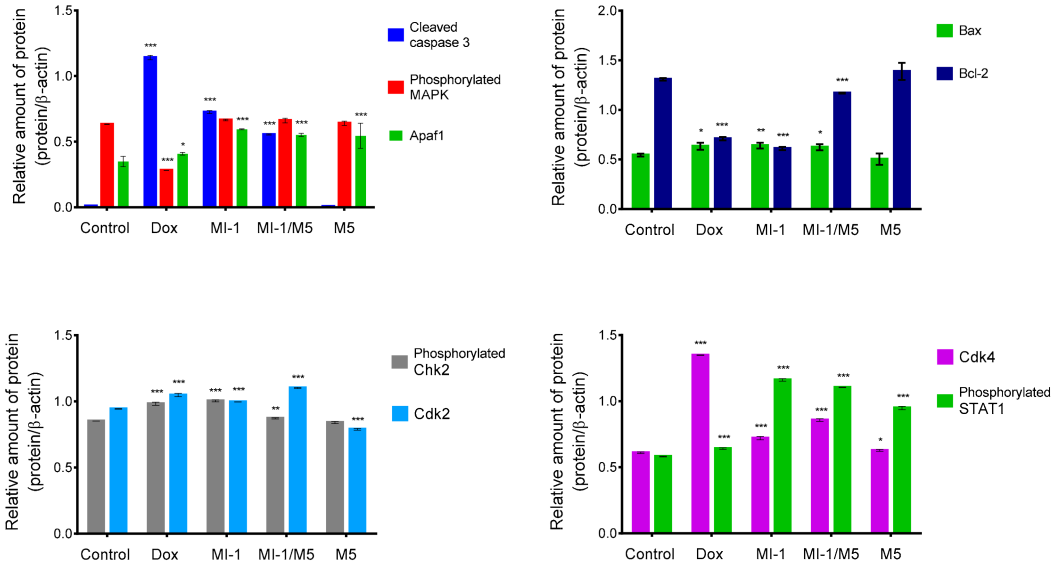

Figure 7. The results of densitometric evaluation of protein content according to Western-blot analysis of proteins of HCT116 cells treated for 48 h with doxorubicin (Dox, 0.9 μg/mL), MI-1 (0.9 μg/mL), MI-1/M5 complex (0.9 μg/mL), and free M5 polymer (0.9 μg/mL). * $p < 0.05$; ** $p < 0.01$; *** $p < 0.001$ compared with control (non-treated) cells.

The MI-1, MI-1/M5 complex, doxorubicin, and M5 polymer increased the amount of cytosolic Apaf1 protein (apoptotic protease-activating factor 1) in HCT116 cells. This protein is a central element of the mitochondrial pathway of apoptosis induced in response to a wide range of the pro-apoptotic factors. The formation of an apoptosome which includes Araf-1, cytochrome c, and initiating pro-caspase 9, is necessary to activate the caspase cascade in cells induced to apoptosis [52].

Mitogen Activated Protein Kinase (MAPK) is a group of protein Serine-Threonine kinases that play an important role in the regulation of cell proliferation and differentiation, as well as in cell survival and drug resistance [53]. The MI-1, its MI-1/M5 complex, and free M5 polymer did not affect the amount of phosphorylated form of the MAPK in HCT116 cells, while doxorubicin significantly inhibited its amount (Figures 6 and 7).

The MI-1, its MI-1/M5 complex, and free M5 polymer increased the content of phosphorylated form of STAT1 in HCT116 cells, while doxorubicin reduced the amount of this protein (Figures 6 and 7). STAT1 is a member of the signal transducer and transcription activators (STAT) family, capable of transmitting a signal from the membrane receptor to the nucleus and DNA. This protein is located predominantly in mitochondria and it is involved in promoting the apoptotic cell death [54]. STAT1 plays a crucial role in the regulation of tumor formation via inducing antiproliferative and pro-apoptotic genes whose products inhibit tumor growth. STAT1 also blocks cell cycle progression and/or inhibits angiogenesis in tumors [54]. Thus, the MI-1 and its MI-1/M5 complex affected the proliferation of HCT116 cells and launched a mitochondria-dependent pathway of apoptosis in these cells through a mechanism of STAT1 signaling.

The MI-1, its MI-1/M5 complex, and doxorubicin increased the content of phosphorylated form of Chk2 (checkpoint kinase 2), cyclin-dependent kinases Cdk2 and Cdk4 in HCT116 cells (Figures 6 and 7). In the G1 phase, the complex of cyclin A with Cdk2 and the complex of cyclin E with Cdk2 in the early S phase regulate the transition of cells from G1 to S phase [55]. After DNA damage, Chk2 protein is phosphorylated which, in turn, inactivates Cdc25A phosphatase. Deactivation of Cdc25A leads to an increase in the phos-

phorylated (inactive) form of Cdk2, therefore, cells cannot enter S phase and replicate their DNA [55]. Based on results of measuring the content of Cdk2, Cdk4, and phosphorylated form of Chk2 in HCT116 cells, one can assume that MI-1, its MI-1/M5 complex affects the transition of cells from G2 to M phase and causes the arrest of cells in the G2/M checkpoint.

3.4. Interaction of MI-1 and Its Complex with DNA

The MI-1 in 1 and 10 μg/mL doses replaced the methyl green dye from the DNA-methyl green complex by 16.5% and 21.2%, respectively (Figure 8), while the MI-1/M5 complex was less active in such a replacement, compared with the MI-1. The MI-1/M5 complex (1 and 10 μg/mL) replaced the methyl green from the DNA-methyl green complex by 7.2% and 6.5%, respectively. The poly(PEGMA-*co*-DMM) (M5) at studied concentrations demonstrated similar low ability to replace the methyl green from the DNA-methyl green complex-5.1% and 6.0% of the replaced methyl green under its action in 1 and 10 μg/mL, respectively. The reference compounds doxorubicin and the Ethidium bromide possessed significantly higher substitution ability (54.1–80.1%) compared with MI-1, MI-1/M5, and M5.

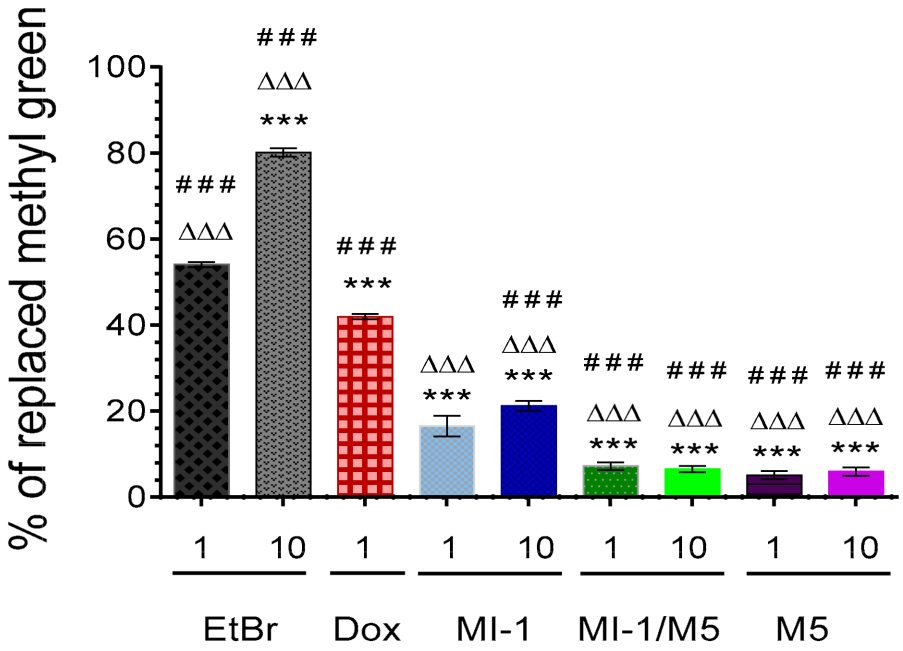

Figure 8. The percentage of methyl green dye replaced from its complex with DNA by the MI-1 (1, 10 μg/mL), MI-1/M5 complex (1, 10 μg/mL), free M5 polymer (1, 10 μg/mL), and reference compounds-doxorubicin (Dox, 1 μg/mL) and Ethidium bromide (EtBr, 1 and 10 μg/mL). *** $p < 0.001$ (significant changes compared with the effect of EtBr (1 μg/mL); $^{\Delta\Delta\Delta}$ $p < 0.001$ (significant changes compared with the effect of Dox (1 μg/mL); $^{\#\#\#}$ $p < 0.001$ significant changes compared with the effect of MI-1 (1 μg/mL). Data are presented as mean ± SD.

Development of the DNA-binding/intercalating anticancer agents is an important approach in chemotherapy improvement [56]. The intercalation of MI-1, its MI-1/M5 complex and free M5 polymer into a DNA molecule was investigated by using adapted method with DNA-tropic dye–the methyl green [27].

3.5. The Damage of DNA Molecule by MI-1 and Its Complex

The DNA interacts with several cellular proteins which leads to strand breaks, chromatid segregation, and cell cycle arrest that affects cell survival [56]. The alkaline comet assay of HCT116 cells revealed single-strand breaks in molecules of nuclear DNA under the action of the MI-1, MI-1/M5 complex, and doxorubicin. The MI-1 caused DNA damage in

HCT116 cells with the Olive Tail Moment (OTM) of 13.2 (Figure 9), and the MI-1/M5 complex caused similar DNA damage in these cells (OTM = 14.0). Free M5 polymer induced minor DNA damage with the OTM of 4.1. The doxorubicin induced OTM at the level of 10.9, while only weak DNA damage (OTM equals 1.8) was detected in the un-treated HCT116 cells (Figure 9).

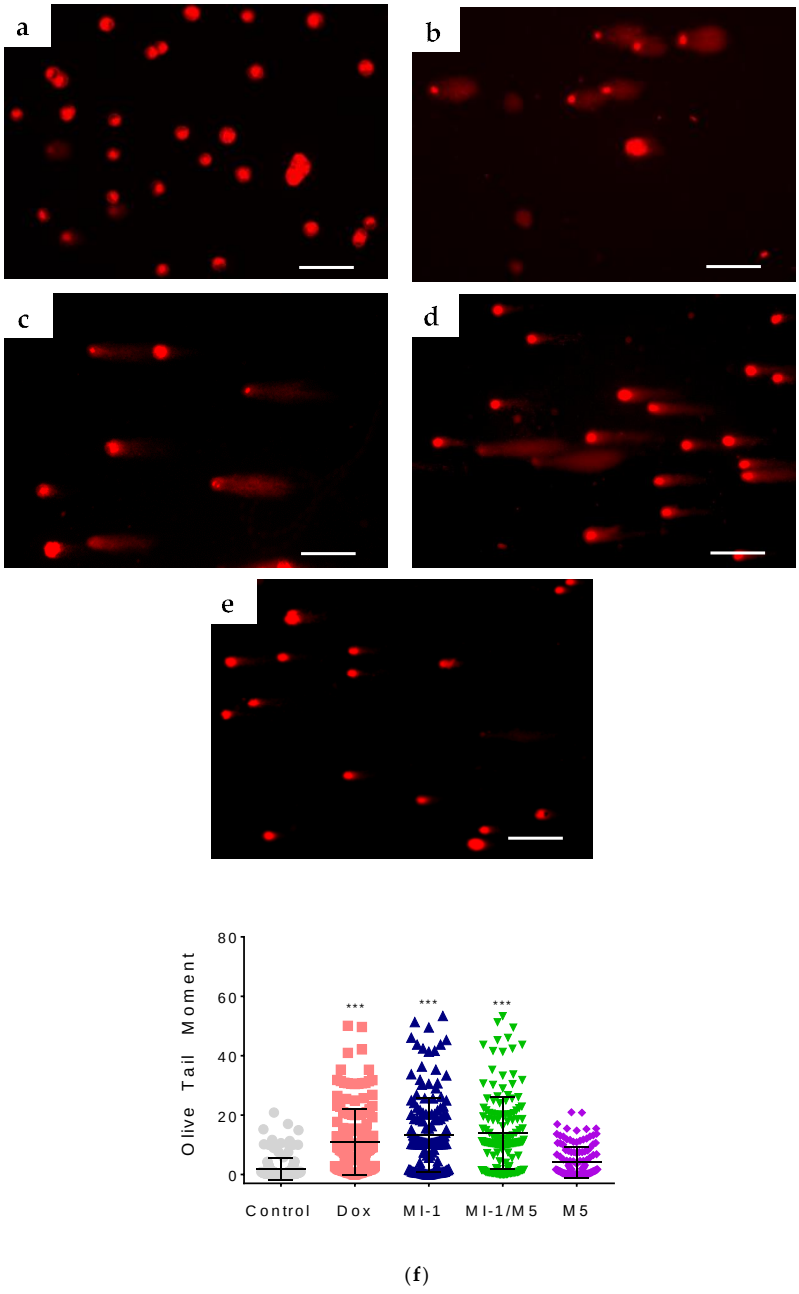

Figure 9. The DNA damage induced by studied compounds in colon carcinoma HCT116 cells (according to the results of alkaline DNA comet assay): (**a**) control; (**b**) doxorubicin (Dox, 0.9 μg/mL); (**c**) MI-1 (0.9 μg/mL); (**d**) complex MI-1/M5 (0.9 μg/mL); (**e**) polymer M5 (0.9 μg/mL); (**f**) quantitative data of DNA damage (Olive Tail Moment) in treated HCT116 cells. *** $p < 0.001$ (significant changes compared with control (non-treated) cells). Scale 50 μm.

The DNA targeting effects were reported for maleimide derivatives RG108 and RG119-1 (1-[2-(1H-Indol-3-yl)-ethyl]-pyrrole-2,5-dione) that possess the DNA methyltransferase inhibition activity [57].

3.6. Morphological Changes in HCT116 Cells Treated with MI-1 and Its Complex

The morphological examination of HCT116 cells treated with studied compounds was conducted by using double staining of chromatin with Hoechst 33342 (blue fluorescence) and Propidium iodide (red fluorescence). The MI-1 compound and MI-1/M5 complex triggered changes in shape of treated cells and their membrane blebbing (marked with white arrows) (Figure 10c–f). Besides, the MI-1 caused chromatin condensation (marked with yellow arrows) and micronuclei formation (marked with pink arrows) (Figure 10c,d). The condensed chromatin and membrane blebbing are typical proapoptotic changes revealed in cells induced to apoptosis [58]. The M5 polymer (Figure 10g,h) and DMSO (Figure 10i,j) did not cause pronounced morphological changes in the treated HCT116 cells.

Thus, complexation of novel kinase inhibitor, namely the maleimide derivative 1-(4-chlorobenzyl)-3-chloro-4-(3-trifluoromethylphenylamino)-1*H*-pyrrole-2,5-dione (MI-1), with the polymeric carrier, poly(PEGMA-*co*-DMM) (M5), permitted achieving two principal aims: (1) creation of a water-soluble form of the MI-1 that facilitates its application in vitro; (2) enhancement of anticancer action of MI-1 towards human tumor cells in vitro with a prevention of its cytotoxic action towards pseudo-normal mammalian cells. The results of exploration of cellular and molecular mechanisms of the cytotoxic effect of the created complex suggest that this effect might be realized via the induction of mitochondria-dependent pathway of apoptosis. It was found that MI-1 and its water-soluble complex triggered proapoptotic morphological changes in treated HCT116 cells, namely chromatin condensation and membrane blebbing, while the action of free polymer did not lead to such cytomorphological changes. Based on the revealed changes in content of Cdk2, Cdk4, and phosphorylated form of Chk2 in HCT116 cells, one can assume that MI-1, its MI-1/M5 complex could affect the transition of cells from G2 to M phase and cause the arrest of these cells in G2/M checkpoint. It was shown that MI-1 decreased S and G2 + M populations with simultaneous increase in G0/G1 population in human osteosarcoma MG-63 cells [24] and in human neoplastic monoblast U-937 cells [28], which is in line with our findings and confirms the suggestion about the impact of MI-1 and MI-1/M5 complex on cell cycling. DNA damage under the action of the MI-1 was also detected, however, it was not enhanced by MI-1 immobilization on the polymeric carrier. The capability of MI-1 and its MI-1/M5 complex to activate caspase 3, together with the above noted increasing in the amount of the phosphorylated form of Chk2, might be responsible for the DNA damage in HCT116 cells. Previously, it was also reported that MI-1 induced apoptosis in MG-63 cells, human ovarian carcinoma SKOV-3 cells [24], as well as in U-937 cells [28]. The level of intercalation of the MI-1 into DNA structure was approximately 50% of such level detected at the action of doxorubicin, and MI-1 complexation with the polymeric carrier almost totally blocked the DNA intercalation effect. Studies are in progress on the therapeutic effect of MI-1 and MI-1/M5 complex in the treatment of Nemeth-Kellner lymphoma (NK/Ly)-bearing mice.

Summarizing, we consider that the poly (PEGMA-*co*-DMM) might be a promising carrier for delivery of the maleimide derivative, MI-1, as well as other biologically active substances with poor water solubility.

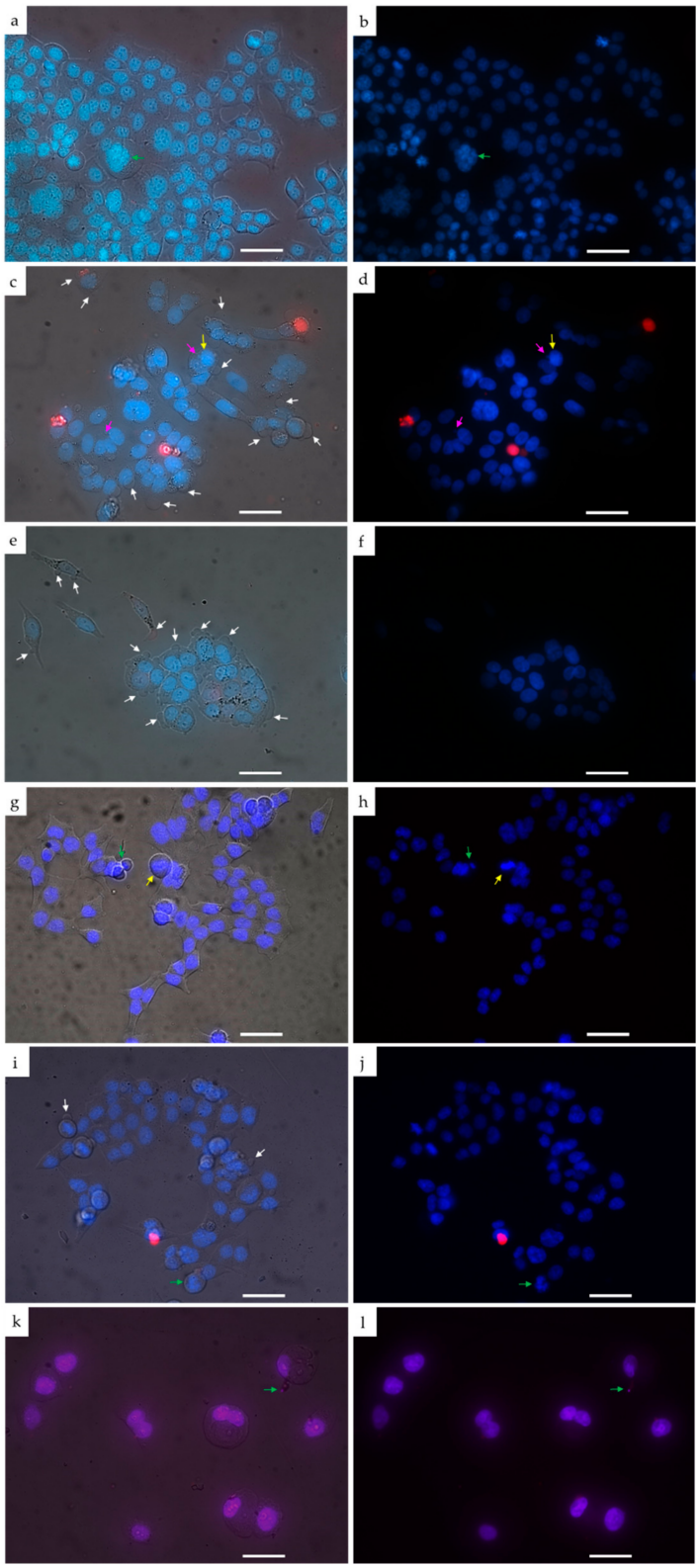

Figure 10. The images of HCT116 cells treated for 48 h with the compounds under study: (**a**,**b**) control; (**c**,**d**) MI-1 compound (1 µg/mL); (**e**,**f**) MI-1/M5 complex (1 µg/mL); (**g**,**h**) free M5 polymer (1 µg/mL); (**i**,**j**) DMSO (1 µg/mL); (**k**,**l**) doxorubicin (0.25 µg/mL). **Left**–differential interference contrast (DIC) images of treated cells stained with Hoechst-33342 and Propidium iodide. **Right**–fluorescent image of treated cells (blue color–staining with Hoechst-33342, red–staining with Propidium iodide). Yellow arrows indicate chromatin condensation, green arrows–chromatin fragmentation, white arrows–plasma membrane blebbing, pink arrows–micronuclei). Scale 20 µm.

4. Conclusions

We found that immobilization of a novel kinase inhibitor, the maleimide derivative 1-(4-chlorobenzyl)-3-chloro-4-(3-trifluoromethylphenylamino)-1*H*-pyrrole-2,5-dione (MI-1), on the poly(PEGMA-*co*-DMM) polymeric carrier (M5) improved significantly the water solubility of the MI-1 and enhanced its toxicity towards human colon (HCT116 and HCT116 p53-/-) and cervical (HeLa) carcinoma and melanoma (SK-MEL-28) cells with GI_{50} value in the range of 0.67–5.43 μg/mL. The *P53* gene status of colon cancer cell did not affect considerably the response of these cells to treatment with the MI-1 and its MI-1/M5 complex. The MI-1 and MI-1/M5 complex showed high selectivity index (SI 6.9) towards studied tumor cell lines, compared with the selectivity of doxorubicin. Free M5 polymer possessed low toxicity towards HCT116, HCT116 p53-/-, SK-MEL-28, HeLa cells. The MI-1/M5 complex inhibited colony formation (characteristics of transformed phenotype) of HCT116 cells more efficiently compared with free MI-1. It should be stressed that growth inhibition of the pseudo-normal HaCaT and Balb/c 3T3 cell lines under the action of the MI-1, MI-1/M5, and free M5 polymer was much weaker (GI_{50} > 50 μg/mL) than such inhibition of tumor cells. The MI-1 and its MI-1/M5 complex induced mitochondria-dependent pathway of apoptosis, caused morphological changes and the DNA damage in HCT116 cells, and affected the transition of these cells from G2 to M phase. While free MI-1 intercalated into the DNA molecule, the MI-1/M5 complex and free M5 polymer possessed significantly lower intercalating ability. Thus, poly (PEGMA-*co*-DMM) can be a promising carrier for delivery of a novel kinase inhibitor, the MI-1.

Author Contributions: Conceptualization, R.S., A.Z. and V.R.; methodology, N.F., R.S., N.M., A.Z., O.K., H.K. and V.R.; investigation, N.F., N.M., A.Z., O.K., H.K. and K.V.; visualization and data analysis, N.F. and O.K.; preparation of original manuscript draft, N.F.; writing—reviewing and editing, R.S., N.M., A.Z., O.K., K.V., H.K. and V.R.; supervision, R.S.; project administration, V.R. All authors have read and agreed to the published version of the manuscript.

Funding: This research received no external funding.

Institutional Review Board Statement: Not applicable.

Informed Consent Statement: Not applicable.

Data Availability Statement: All data generated during this research are presented in the manuscript.

Acknowledgments: The authors thank Walter Berger (Institute of Cancer Research, Medical University of Vienna, Vienna, Austria) for kind donating of human colon carcinoma HCT116 p53-/- cells.

Conflicts of Interest: The authors declare no conflict of interest.

References

1. Olgen, S. Overview on anticancer drug design and development. *Curr. Med. Chem.* **2018**, *25*, 1704–1719. [CrossRef] [PubMed]
2. Ali, I.; Lone, M.N.; Aboul-Enein, H.Y. Imidazoles as potential anticancer agents. *MedChemComm* **2017**, *8*, 1742–1773. [CrossRef] [PubMed]
3. Narvekar, M.; Xue, H.Y.; Eoh, J.Y.; Wong, H.L. Nanocarrier for poorly water-soluble anticancer drugs-barriers of translation and solutions. *AAPS PharmSciTech* **2014**, *15*, 822–833. [CrossRef] [PubMed]
4. Ferrari, R.; Sponchioni, M.; Morbidelli, M.; Moscatelli, D. Polymer nanoparticles for the intravenous delivery of anticancer drugs: The checkpoints on the road from the synthesis to clinical translation. *Nanoscale* **2018**, *10*, 22701–22719. [CrossRef]
5. Majumder, N.; Das, N.G.; Das, S.K. Polymeric micelles for anticancer drug delivery. *Ther. Deliv.* **2020**, *11*, 613–635. [CrossRef]
6. Duchene, D.; Cavalli, R.; Gref, R. Cyclodextrin-based polymeric nanoparticles as efficient carriers for anticancer drugs. *Curr. Pharm. Biotechnol.* **2016**, *17*, 248–255. [CrossRef]
7. Sun, H.; Yarovoy, I.; Capeling, M.; Cheng, C. Polymers in the co-delivery of siRNA and anticancer drugs for the treatment of drug-resistant cancers. *Top. Curr. Chem.* **2017**, *375*, 24. [CrossRef]
8. Rizwanullah, M.; Alam, M.; Harshita, M.S.R.; Rizvi, M.M.; Amin, S. Polymer-lipid hybrid nanoparticles: A next-generation nanocarrier for targeted treatment of solid tumors. *Curr. Pharm. Des.* **2020**, *26*, 1206–1215. [CrossRef]
9. Oliveira, A.L.C.d.L.; Schomann, T.; de Geus-Oei, L.F.; Kapiteijn, E.; Cruz, L.J.; de Araújo, R.F., Jr. Nanocarriers as a tool for the treatment of colorectal cancer. *Pharmaceutics* **2021**, *13*, 1321. [CrossRef]
10. Paris, C.; Brun, O.; Pedroso, E.; Grandas, A. Exploiting protected maleimides to modify oligonucleotides, peptides and peptide nucleic acids. *Molecules* **2015**, *20*, 6389–6408. [CrossRef]

11. Ravasco, J.M.J.M.; Faustino, H.; Trindade, A.; Gois, P.M.P. Bioconjugation with maleimides: A useful tool for chemical biology. *Chemistry* **2019**, *25*, 43–59. [CrossRef] [PubMed]
12. Shi, Q.; Zhang, Y.; Huang, Z.; Zhou, N.; Zhang, Z.; Zhu, X. Precise sequence regulation through maleimide chemistry. *Polym. J.* **2020**, *52*, 21–31. [CrossRef]
13. Muthyala, M.K.K.; Sahoo, S.K.; Nagasree, K.P.; Pemmadi, R.V.; Jamullamudi, R.N. Synthesis and screening of new maleimide derivatives as potential anti-tubercular agents. *J. App. Pharm. Sci.* **2015**, *5*, 44–47. [CrossRef]
14. Matuszak, N.; Muccioli, G.G.; Labar, G.; Lambert, D.M. Synthesis and in vitro evaluation of N-substituted maleimide derivatives as selective monoglyceride lipase inhibitors. *J. Med. Chem.* **2009**, *52*, 7410–7420. [CrossRef]
15. Pajak, B.; Orzechowska, S.; Gajkowska, B.; Orzechowski, A. Bisindolylmaleimides in anti-cancer therapy—More than PKC inhibitors. *Adv. Med. Sci.* **2008**, *53*, 21–31. [CrossRef] [PubMed]
16. Liu, W.; Beck, J.; Schmidt, L.C.; Roolf, C.; Pews-Davtyan, A.; Rütgen, B.C.; Hammer, S.; Willenbrock, S.; Sekora, A.; Rolfs, A.; et al. Characterization of the novel indolylmaleimides' PDA-66 and PDA-377 effect on canine lymphoma cells. *Oncotarget* **2016**, *7*, 35379–35389. [CrossRef]
17. Van Eis, M.J.; Evenou, J.; Schuler, W.; Zenke, G.; Vangrevelinghe, E.; Wagner, J.; von Matt, P. Indolyl-naphthylmaleimides as potent and selective inhibitors of protein kinase C-a/b. *Bioorg. Med. Chem Lett.* **2017**, *27*, 781–786. [CrossRef]
18. Esfandyari-Manesh, M.; Abdi, M.; Talasaz, A.H.; Ebrahimi, S.M.; Atyabi, F.; Dinarvand, R. S2P peptide-conjugated PLGA-maleimide-PEG nanoparticles containing imatinib for targeting drug delivery to atherosclerotic plaques. *DARU J. Pharm. Sci.* **2020**, *28*, 131–138. [CrossRef]
19. Pichler, V.; Mayr, J.; Heffeter, P.; Dömötör, O.; Enyedy, É.A.; Hermann, G.; Groza, D.; Köllensperger, G.; Galanksi, M.; Berger, W.; et al. Maleimide-functionalised Platinum(IV) complexes as a synthetic platform for targeted drug delivery. *Chem. Commun.* **2013**, *49*, 2249–2251. [CrossRef]
20. Gutowski, S.M.; Shoemaker, J.T.; Templeman, K.L.; Wei, Y.; Latour, R.A., Jr.; Bellamkonda, R.V.; LaPlaca, M.C.; García, A.J. Protease-degradable PEG-maleimide coating with on-demand release of IL-1Ra to improve tissue response to neural electrodes. *Biomaterials* **2015**, *44*, 55–70. [CrossRef]
21. Hu, S.-M.; Lee, C.-Y.; Chang, Y.-M.; Xiao, J.-Q.; Kusanagi, T.; Wu, T.-Y.; Chang, N.-Y.; Christy, J.; Chiu, Y.-R.; Huang, C.-W.; et al. Vapor-phase fabrication of a maleimide-functionalized poly-*p*-xylylene with a three-dimensional structure. *Coatings* **2021**, *11*, 466. [CrossRef]
22. Lee, W.J.; Cha, S.H. Improvement of mechanical and self-healing properties for polymethacrylate derivatives containing maleimide modified graphene oxide. *Polymers* **2020**, *12*, 603. [CrossRef]
23. Dubinina, G.G.; Chupryna, O.O.; Platonov, M.O.; Borisko, P.O.; Ostrovska, G.V.; Tolmachov, A.O.; Shtil, A.A. In silico design of protein kinase inhibitors: Successes and failures. *Anticancer Agents Med. Chem.* **2007**, *7*, 171–188. [CrossRef]
24. Kuznietsova, H.; Dziubenko, N.; Byelinska, I.; Hurmach, V.; Bychko, A.; Lynchak, O.; Milokhov, D.; Khilya, O.; Rybalchenko, V. Pyrrole derivatives as potential anti-cancer therapeutics: Synthesis, mechanisms of action, safety. *J. Drug Target.* **2020**, *28*, 547–563. [CrossRef]
25. Kuznietsova, H.M.; Yena, M.S.; Kotlyar, I.P.; Ogloblya, O.V.; Rybalchenko, V.K. Anti-inflammatory effects of protein kinase inhibitor pyrrol derivate. *Sci. World J.* **2016**, *2016*, 2145753. [CrossRef]
26. Dubinina, G.; Golovach, S.; Kozlovsky, V.; Tolmachov, A.O.; Volovenko, Y.M. Antiproliferative action of the new derivatives of l-(4-R-benzyl)-3-R1-4-(R2-phenylamino)-1H-pyrrol-2,5-dione. *Zurn. Organ. Farmacevt. Khimi* **2007**, *5*, 39–49. (In Ukrainian)
27. Finiuk, N.S.; Ivasechko, I.I.; Klyuchivska, O.Y.; Kuznietsova, H.M.; Rybalchenko, V.K.; Stoika, R.S. Cytotoxic action of maleimide derivative 1-(4-Cl-benzyl)-3-chloro-4-(CF(3)-phenylamino)-1H-pyrrole-2,5-dione toward mammalian tumor cells and its capability to interact with DNA. *Ukr. Biochem. J.* **2020**, *92*, 55–62. [CrossRef]
28. Byelinska, I.V.; Garmanchuk, L.V.; Khranovska, N.M.; Shelest, D.V.; Rybalchenko, T.V. Effect of maleimide derivative, protein kinases inhibitor, on the morphofunctional state of human neoplastic monoblast cell line U-937. *Res. J. Pharm. Biol. Chem. Sci.* **2016**, *7*, 1898–1905.
29. Kuznietsova, H.M.; Lynchak, O.V.; Danylov, M.O.; Kotliar, I.P.; Rybalchenko, V.K. Effect of dihydropyrrol and maleimide derivatives on the state of liver and colon in normal rats and those with colorectal carcinogenesis induced by dimethylhydrazine. *Ukr. Biochem. J.* **2013**, *85*, 74–84. [CrossRef]
30. Kuznietsova, H.M.; Luzhenetska, V.K.; Kotlyar, I.P.; Rybalchenko, V.K. Effects of 5-amyno-4-(1,3-benzothyazol-2-yn)-1-(3-methoxyphenyl)-1,2-dihydro-3H- pyrrole-3-one intake on digestive system in a rat model of colon cancer. *Sci. World J.* **2015**, *2015*, 376576. [CrossRef] [PubMed]
31. Bielins'ka, I.V.; Lynchak, O.V.; Rybal'chenko, T.V.; Hurniak, O.M. Hematological effects of the protein kinase inhibitor maleimide derivative in dimethylhydrazin E-induced colorectal carcinogenesis of rats. *Fiziolohichnyi Zhurnal* **2014**, *60*, 40–49. (In Ukrainian) [CrossRef]
32. Byelinska, I.V.; Lynchak, O.V.; Tsyvinska, S.M.; Rybalchenko, V.K. Morphofunctional state of blood cells after chronic exposure of the protein kinases inhibitor maleimide derivative. *Fiziolohichnyi Zhurnal* **2015**, *61*, 71–77. (In Ukrainian) [CrossRef]
33. Finiuk, N.S.; Popovych, M.V.; Shalai, Y.R.; Mandzynets, S.M.; Hreniuh, V.P.; Ostapiuk, Y.V.; Obushak, M.D.; Mitina, N.E.; Zaichenko, O.S.; Stoika, R.S.; et al. Antineoplastic activity in vitro of 2-amino-5-benzylthiasol derivative in the complex with nanoscale polymeric carriers. *Cytol. Genet.* **2021**, *55*, 19–27. [CrossRef]

34. Kuznietsova, H.M.; Hurmach, V.V.; Bychko, A.V.; Tykhoniuk, O.I.; Milokhov, D.S.; Khilya, O.V.; Volovenko, Y.M.; Rybalchenko, V.K. Synthesis and biological activity of 4-amino-3-chloro-1H-pyrrole-2,5-diones. *In Silico Pharmacol.* **2019**, *7*, 2. [CrossRef]
35. Paiuk, O.L.; Mitina, N.Y.; Kinash, N.I.; Yakymovych, A.B.; Hevus, O.I.; Zaichenko, A.S. Comb-like polyethylene glycol containing oligomeric surfactants with reactive terminal groups. *Ukr. Chem. J.* **2018**, *84*, 1–9. (In Ukrainian) [CrossRef]
36. Francuskiewicz, F. *Polymer Fractionation*; Springer: Berlin/Heidelberg, Germany, 1994; p. 217. ISBN 978-3-642-78704-1.
37. Mitina, N.Y.; Riabtseva, A.O.; Garamus, V.M.; Lesyk, R.B.; Volyanyuk, K.A.; Izhyk, O.M.; Zaichenko, O.S. Morphology of the micelles formed by a comb-like PEG-containing copolymer loaded with antitumor substances with different water solubilities. *Ukr. J. Phys.* **2020**, *65*, 670. [CrossRef]
38. Finiuk, N.; Klyuchivska, O.; Ivasechko, I.; Hreniukh, V.; Ostapiuk, Y.; Shalai, Y.; Panchuk, R.; Matiychuk, V.; Obushak, M.; Stoika, R.; et al. Proapoptotic effects of novel thiazole derivative on human glioma cells. *Anticancer Drugs* **2019**, *30*, 27–37. [CrossRef] [PubMed]
39. NÚÑez, J.G.; Pinheiro, J.S.; Padilha, G.L.; Garcia, H.O.; Porta, V.; Apel, M.A.; Bruno, A.N. Antineoplastic potential and chemical evaluation of essential oils from leaves and flowers of *Tagetes ostenii* Hicken. *An. Acad. Bras. Cienc.* **2020**, *92*, e20191143. [CrossRef] [PubMed]
40. Mahmood, T.; Yang, P.C. Western blot: Technique, theory, and trouble shooting. *N. Am. J. Med. Sci.* **2012**, *4*, 429–434. [CrossRef] [PubMed]
41. Gallo-Oller, G.; Ordoñez, R.; Dotor, J. A new background subtraction method for Western blot densitometry band quantification through image analysis software. *J. Immunol. Methods* **2018**, *457*, 1–5. [CrossRef] [PubMed]
42. Dabiri, Y.; Abu El Maaty, M.A.; Chan, H.Y.; Wölker, J.; Ott, I.; Wölfl, S.; Cheng, X. p53-dependent anti-proliferative and pro-apoptotic effects of a gold(I) N-heterocyclic carbene (NHC) complex in colorectal cancer cells. *Front. Oncol.* **2019**, *9*, 438. [CrossRef]
43. Abu El Maaty, M.A.; Strassburger, W.; Qaiser, T.; Dabiri, Y.; Wölfl, S. Differences in p53 status significantly influence the cellular response and cell survival to 1,25-dihydroxyvitamin D3-metformin cotreatment in colorectal cancer cells. *Mol. Carcinog.* **2017**, *56*, 2486–2498. [CrossRef] [PubMed]
44. Hayashi, Y.; Tsujii, M.; Kodama, T.; Akasaka, T.; Kondo, J.; Hikita, H.; Inoue, T.; Tsujii, Y.; Maekawa, A.; Yoshii, S.; et al. p53 functional deficiency in human colon cancer cells promotes fibroblast-mediated angiogenesis and tumor growth. *Carcinogenesis* **2016**, *37*, 972–984. [CrossRef]
45. Boyer, J.; McLean, E.G.; Aroori, S.; Wilson, P.; McCulla, A.; Carey, P.D.; Longley, D.B.; Johnston, P.G. Characterization of p53 wild-type and null isogenic colorectal cancer cell lines resistant to 5-fluorouracil, oxaliplatin, and irinotecan. *Clin. Cancer Res.* **2004**, *10*, 2158–2167. [CrossRef] [PubMed]
46. García, A.J. PEG-maleimide hydrogels for protein and cell delivery in regenerative medicine. *Ann. Biomed. Eng.* **2014**, *42*, 312–322. [CrossRef] [PubMed]
47. Segun, P.A.; Ogbole, O.O.; Ismail, F.M.D.; Nahar, L.; Evans, A.R.; Ajaiyeoba, E.O.; Sarker, S.D. Resveratrol derivatives from *Commiphora africana* (A. Rich.) Endl. display cytotoxicity and selectivity against several human cancer cell lines. *Phytother. Res.* **2019**, *33*, 159–166. [CrossRef] [PubMed]
48. Da'i, M.; Meilinasary, K.A.; Suhendi, A.; Haryanti, S. Selectivity index of *Alpinia galanga* extract and 1′-acetoxychavicol acetate on cancer cell lines. *Indones. J. Cancer Chemoprevent.* **2019**, *10*, 95–100.
49. Beaver, C.M. The effect of culture conditions on colony morphology and proliferative capacity in human prostate cancer cell lines. *Cell Biol. Toxicol.* **2012**, *28*, 291–301. [CrossRef]
50. McIlwain, D.R.; Berger, T.; Mak, T.W. Caspase functions in cell death and disease. *Cold Spring Harb. Perspect. Biol.* **2013**, *5*, a008656. [CrossRef]
51. Ngoi, N.; Choong, C.; Lee, J.; Bellot, G.; Wong, A.; Goh, B.C.; Pervaiz, S. Targeting mitochondrial apoptosis to overcome treatment resistance in cancer. *Cancers* **2020**, *12*, 574. [CrossRef]
52. Yoshida, H.; Kong, Y.Y.; Yoshida, R.; Elia, A.J.; Hakem, A.; Hakem, R.; Penninger, J.M.; Mak, T.W. Apaf1 is required for mitochondrial pathways of apoptosis and brain development. *Cell* **1998**, *94*, 739–750. [CrossRef]
53. Lu, M.; Wang, Y.; Zhan, X. The MAPK pathway-based drug therapeutic targets in pituitary adenomas. *Front. Endocrinol.* **2019**, *10*, 330. [CrossRef] [PubMed]
54. Zhang, Y.; Liu, Z. STAT1 in cancer: Friend or foe? *Discov. Med.* **2017**, *24*, 19–29. [PubMed]
55. Topacio, B.R.; Zatulovskiy, E.; Cristea, S.; Xie, S.; Tambo, C.S.; Rubin, S.M.; Sage, J.; Kõivomägi, M.; Skotheim, J.M. Cyclin D-Cdk4,6 drives cell-cycle progression via the retinoblastoma protein's c-terminal helix. *Mol. Cell.* **2019**, *74*, 758–770. [CrossRef]
56. Baguley, B.C.; Drummond, C.J.; Chen, Y.Y.; Finlay, G.J. DNA-binding anticancer drugs: One target, two actions. *Molecules* **2021**, *26*, 552. [CrossRef]
57. Rondelet, G.; Fleury, L.; Faux, C.; Masson, V.; Dubois, J.; Arimondo, P.B.; Willems, L.; Wouters, J. Inhibition studies of DNA methyltransferases by maleimide derivatives of RG108 as non-nucleoside inhibitors. *Future Med. Chem.* **2017**, *9*, 1465–1481. [CrossRef] [PubMed]
58. Elmore, S. Apoptosis: A review of programmed cell death. *Toxicol. Pathol.* **2007**, *35*, 495–516. [CrossRef]